

Analysis of visible light images from a fast-gated intensified charge coupled device camera during flux rope interaction and magnetic reconnection

E. Hemsing,^{a)} I. Furno, and T. Intrator

Los Alamos National Laboratory, M.S. E526, Los Alamos, New Mexico 87545

D. Wei

Massachusetts Institute of Technology, Cambridge, Massachusetts 02139

(Presented on 21 April 2004; published 12 October 2004)

We present the experimental setup and analysis of visible light images from a fast double-gated intensified charge coupled device (CCD) camera currently being used on the reconnection scaling experiment (RSX) at the Los Alamos National Laboratory. In RSX, externally driven free-boundary flux ropes are generated for magnetic reconnection studies in collisional plasma. Time-resolved images of flux rope interaction on submicrosecond time scales are achieved through the use of a microchannel plate intensified CCD camera and are shown to be consistent with probe measurements of plasma pressure and magnetic structure. High experimental repeatability allows plasma evolution to be displayed and measured from images taken over hundreds of RSX discharges to elucidate flux rope interaction dynamics. Peak-intensity fit algorithms extrapolate rope separation and two-dimensional rope velocities from images in agreement with probe data. First glimpses of two flux ropes that twist and merge are presented.

© 2004 American Institute of Physics. [DOI: 10.1063/1.1787169]

I. INTRODUCTION

Precise nonperturbative measurements of plasma evolution and magnetic flux inflow are vital for the study and characterization of magnetic reconnection in laboratory plasmas. In the reconnection scaling experiment (RSX),¹ parallel current-carrying plasma columns, or flux ropes, are generated to experimentally model naturally occurring rope driven reconnection dynamics much like those observed in solar arcades and prominences. Filamentary-shaped plasmas² are free to evolve through mutual or self-interaction and can exhibit complex three-dimensional (3D) behavior. During reconnection in RSX, the flux ropes can pinch, merge, and twist on microsecond time scales, stipulating the need for fast time-resolved imaging techniques.

To externally view the hydrogen plasma, a Cooke Di-Cam intensified charge coupled device (CCD) camera³ with ultraviolet to near-infrared spectral sensitivity is positioned with a lateral view into the chamber (Fig. 1) to collect high-resolution 12-bit images of unfiltered plasma emission. Digitally stored images are used to establish shot-to-shot repeatability and resolve pinch velocities during reconnection. Images are processed with peak intensity fitting routines to locate each flux rope center. Combined with external measurements of current and guide field, we extract information on reconnection flux inflow. Results from this method are presented and compared with velocity data from *in situ* measurements. The imaging technique presented has the distinct experimental advantage of illuminating global rope evolution

in fewer shots than are needed for diagnostic probe scans. As a result, demands on routine maintenance are relaxed and the effective lifetime of the experiment is lengthened.

II. RECONNECTION SCALING EXPERIMENT EXPERIMENTAL SETUP

A 3D reconnection geometry is established with two parallel flux ropes generated by radially inserted plasma guns into an electrically floating 10^{-6} Torr vacuum chamber (Figs. 1 and 2). Inside each gun, an arc discharge ionizes the supply gas. One millisecond later, the gun anodes are biased negatively ($V_{\text{bias}} \leq 300$ V) with respect to an external anode (electrically isolated from the chamber wall) positioned 0.15–3.5 m down the axis of the chamber. Each 1–2 cm radius flux rope carries ≤ 1.3 kA peak current, stabilized during the initial linear current ramp by a reversible, axial guide field ($B_z = 0$ –0.1 T) that remains constant throughout the shot. The Lorentz force between the columns causes them to attract, and later in time, twist around each other. Magnetic reconnection is studied during this initial phase when experimental shot-to-shot reproducibility is high. This allows precise 3D measurements of plasma and field parameters using multiple discharges. Later in the evolution, repeatability is reduced as current exceeds stability thresholds and flux ropes show a high degree of twisting, forming complex helical and spiral structures. Typically, plasmas are scanned with magnetic (B dots), Rogowski⁴ or electrostatic probes inserted radially into the chamber that provide local time-resolved measurements in the xy plane at different z positions (Fig. 2).

^{a)}Electronic mail: ehemsing@lanl.gov

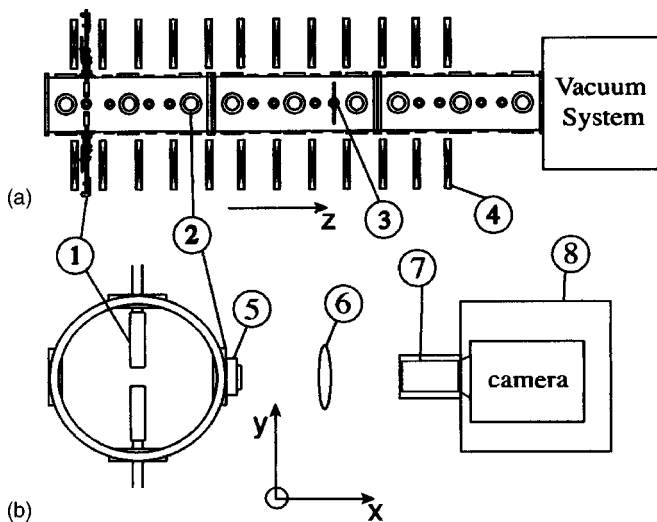


FIG. 1. Reconnection scaling experiment: (a) Side view: Plasma guns are inserted radially and discharge parallel to the cylindrical chamber axis. (1) plasma guns, (2) CCD viewport, (3) external anode, and (4) magnet coil. (b) End-on view: (5) 35 mm wide angle lens, (6) magnifying lens, (7) telephoto attachment, and (8) magnetic shield housing.

III. CAMERA SETUP

In-depth technical specifications on the DiCam-Pro can be found online at <http://www.techimaging.com/products-UHS-DC.html>. Typically, the camera³ is positioned 1 m from the main chamber with a lateral view (Fig. 3) through a 4 in. port window. However, by positioning the camera end on, a full axial view of the plasma can be obtained (Fig. 4). The camera is mounted and shielded from ambient pulsed magnetic fields inside a 51 cm \times 41 cm \times 18 cm Hoffman Type 12 steel enclosure. The box has been modified to include a cooling fan, uninterrupted power supply, rear fiber optic and Standard Bayonet Neill Concelman (BNC) access port, 12 V dc power supply, and a lens shield. At moderate pulsed field strengths ($B_z \leq 200$ G), the enclosure is sufficient to protect the camera even while positioned end on. For higher guide field images that require a wide viewing angle of the plasma, a series of free mounted lenses are preferred for a displaced lateral camera position.

For the high-field setup, a Tamron SF 17 mm 1:3.5 wide angle lens with a 104° viewing angle is positioned against the chamber window, 20 cm from the plasma (Fig. 1). The lens is designed to produce a flat-field wide angle image as opposed to a more distorted, fish-eye view. A 10 cm diam-

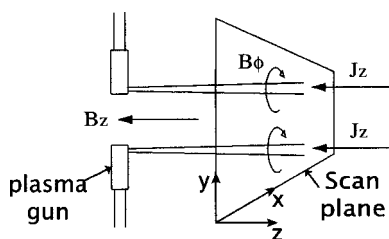


FIG. 2. Plasma gun orientation (side view): Parallel current channels are generated via simultaneously discharging plasma guns. Between them, oppositely directed magnetic field lines are forced together during reconnection. An xy plane is swept out by magnetic probes during scans of the reconnection region.

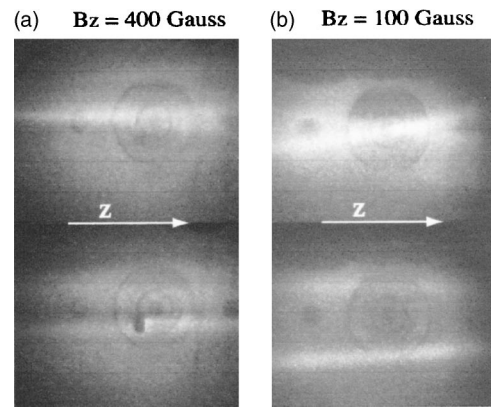


FIG. 3. Two channels are distinguishable while stabilized by a 400 G axial field (left) in the lower image before they appear to merge or visibly overlap in the upper picture $5 \mu\text{s}$ later. A Rogowski probe is visibly illuminated by the lower current channel. Under low guide field ($B_z=100$ G), the right image shows two distinct flux ropes that later helically twist as the current increases. Images above were taken with a 400 ns gate.

eter, 30 cm focal length convex lens magnifies the wide angle image(6). Mounted to the camera is an AF Nikkor 70-210 mm Nikon zoom lens with a $1.6\times$ AF TC-16A tele-converter(7). This configuration results in a depth of focus of 5 cm.

Data transfer is done via fiber optic link through two Leoni Q-line 1G50/125 10 m long optical fiber cables to a Peripheral Component Interconnect bus compatible card with 132 MByte/s burst rate. Triggers are either high speed Transistor-Transistor Logic through a BNC connection or optical through fibers. Likewise, gating can be either BNC or optical for a minimum 20 ns exposure time in two-shot full resolution (1280×1024 SVGA) mode. The camera comes with software that allows automultitriggering and real-time display facilitating easy camera focus and alignment.

IV. IMAGE ANALYSIS

Results are presented from a $B_z=200$ G operating regime from images [see Fig. 5(c) for a few examples] taken throughout the repeatable reconnection phase, ($t=[1.488, 1.500]$ ms). Due to moderate/low guide field, the free-mounted lens setup is not required and the images used for this analysis were taken using only the Nikon zoom lens

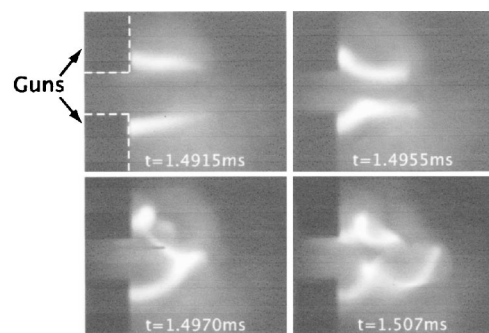


FIG. 4. End on images of rope evolution yield a global perspective of dynamic evolution. Initially parallel ropes early in time begin to merge, later going unstable, and twisting. Plasma ropes are "stuck" by current flow to the gun nozzle seen silhouetted in the foreground, but can drift around the large anode 1 m down the z axis.

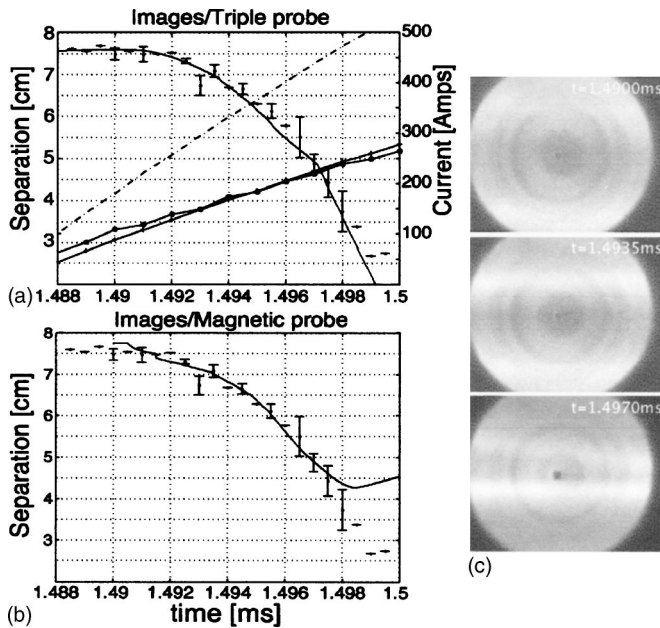


FIG. 5. Rope separation during reconnection extracted from image analysis of lateral view. Comparison of results with triple probe (solid line - plot a) data and magnetic probe data (solid line - plot b) are plotted. Current at the external anode (dashed line) and through each gun is shown for reference. (c) The evolution of ropes during pinch.

and teleconverter mounted directly to the camera. Rope center and separation are extracted from peak intensity scans of each image. Calibration of pixels per centimeter is done using the known dimensions of the *in situ* probes. Figures 5(a) and 5(b) show separation from analysis of 23 pairs of images taken with a $4\ \mu\text{s}$ interframe delay and 200 ns gate time compared with data from internal probes. Image data are plotted with error bars that show the deviation of the rope position over two shots from the peak intensity fit routine. For comparison, electrostatic probe data are assembled from over 180 shots with a high-resolution scan ($5\ \text{mm} \times 5\ \text{mm}$) of density, temperature, and floating potential. From this, we extract the local plasma pressure maxima and identify these as the center of each rope. This separation is calculated and plotted as a solid line [Fig. 5(a)] and shows good agreement with image results. The small probe tip separation ($\leq 2\ \text{mm}$) of the triple probe results in high-resolution two-dimensional (2D) maps of pressure, but demands a large number of discharges to cover the $8\ \text{cm} \times 4\ \text{cm}$ region.

A comparison with a magnetic probe is also plotted as a solid line over the image data [Fig. 5(b)]. Small ($3\ \text{mm} \times 3\ \text{mm} \times 2\ \text{mm}$) commercial inductors in the B dot are arranged to extract 2D changes in magnetic field (B_x, B_y) with a spatial resolution of $5 \times 5\ \text{mm}$ per dimension. The inductors span an effective length about 2 cm so complete scans can be done with fewer shots (30–50). The magnetic probe,

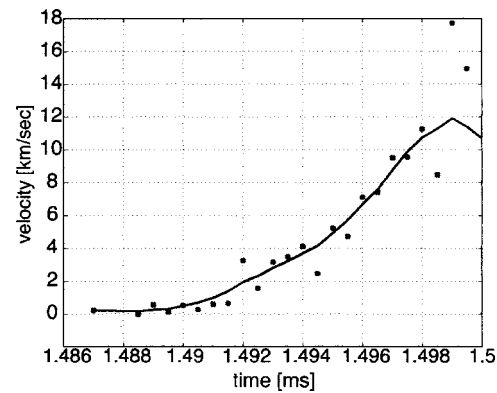


FIG. 6. Inflow velocity toward X point calculated as a function of rope center separation over time.

however, cannot resolve the magnetic structure at zero or very low current. Discrepancies early in time are owed to this lack of sensitivity. Agreement between image analysis and B dot data processing methods diverges at roughly $t = 1.497\ \text{ms}$ because, unlike the magnetic probes, the camera cannot resolve motion along its viewing axis. As the ropes twist, the projected separation as seen by the camera approaches zero whereas the total separation remains significant. Corrections can be made to the inflow using probe data to compensate for the evolution in 3D. During the initial current ramp, however, the motion is dominantly 2D and can be evaluated with images alone. It is during this time that reconnection is studied so the imaging method can be used effectively.

Flux rope pinch velocity is shown in Fig. 6, calculated from images. For velocity calculations, additional effects become important such as the uncertainty in position caused by the nonzero gate time. Images from this set of data were taken with a 200 ns gate, so the blurring is negligible for the velocities shown. Results show sub-Alfvenic velocities where $v_{\text{pinch}} \leq 0.1 v_{\text{Alfven}}$ with respect to B_z .

In conclusion, an intensified fast CCD camera can be used effectively to reveal macroscopic dynamics of flux rope interaction during reconnection in hydrogen plasma. Twisting and merging of free-boundary flux ropes has been shown, with velocities that concur with results from *in situ* diagnostic probes. Image analysis provides a noninvasive acquisition method that reduces the number of required pulsed discharges that can shorten the life of a laboratory experiment. Future plans call for use of two cameras in a stereo-optical configuration to resolve 3D behavior.

¹I. Furno, Rev. Sci. Instrum. **74**, 2324 (2003).

²P. Bellan, Phys. Plasmas **10**, 1999 (2003).

³C. Corp., <http://www.techimaging.com/products-UHS-DC.html> (2003).

⁴E. Torbert, Rev. Sci. Instrum. **74**, 5097 (2003).